



# The influence of alkali-free and alkaline shotcrete accelerators within cement systems

## Influence of the temperature on the sulfate attack mechanisms and damage

C. Paglia<sup>a,\*</sup>, F. Wombacher<sup>b</sup>, H. Böhni<sup>a</sup>

<sup>a</sup>*Institute of Materials Chemistry and Corrosion, Swiss Federal Institute of Technology, Einsteinstrasse, 8093 Honggerberg, Zurich, Switzerland*

<sup>b</sup>*Admixture Department, Central R&D, SIKA AG, Tüffenwies 16-22, 8048 Zurich, Switzerland*

Received 20 September 2000; accepted 13 August 2002

### Abstract

The resistance to sulfate attack of mixtures accelerated with alkali-free and alkaline accelerators was found to be mainly influenced by the  $\text{Al}^{3+}$  and  $\text{SO}_4^{2-}$  added via the admixtures. Microstructural observations showed decalcification and disintegration of the CSH gel, which acted as an additional  $\text{Ca}^{2+}$  supplier as compared to the CH for ettringite formation. The CSH decalcification was mainly observed with a homogeneous distribution of the alkali-free admixture. The disintegration of the CSH gel increased the porosity and allowed more sulfate solution to penetrate into the specimens. This process promoted the swelling of the specimens and directly contributed to the expansion, explaining the lack of a direct relationship between the ettringite formation and the expansion. Moreover, the CSH gel disintegration, typical for  $\text{MgSO}_4$  attack, also occurred with  $\text{Na}_2\text{SO}_4$  solutions and depending on the aluminate–sulfate distribution and the extent of the CSH gel disintegration, different damage types were detected. At higher temperatures (65 °C) the damage was mainly controlled by the growth, the rearrangement and the thermal stability of ettringite.

© 2002 Elsevier Science Ltd. All rights reserved.

*Keywords:* Durability; Accelerators; CSH gel; Ettringite; Temperature

### 1. Introduction

In the shotcrete technology, the new high-performance alkali-free admixtures increasingly substitute the alkali-rich accelerators in order to improve the performance and working safety [1,2], so that the knowledge of the sulfate resistance of both types of admixtures is necessary and becomes the main goal of this work.

It is generally believed that the content of aluminum and sulfate of the alkali-free admixtures may influence the rate of sulfate attack promoting an internal form of attack. Internal sulfate attack has also been correlated with the presence of sulfate-rich constituents in the mixtures [3,4],

with the cement type [5], the dosage [3] and the sulfate present in the clinkers [6]. It is therefore important to determine to which extent the internal sulfate attack may worsen the sulfate resistance of the new alkali-free accelerated systems and to compare these latter systems with the alkali-rich one.

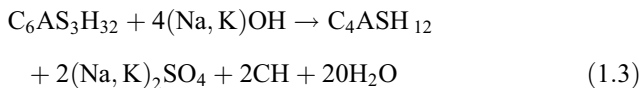
Furthermore, an attempt is made to clarify the contribution of gypsum and ettringite to the extent of the damage and expansion. In this context, the confined crystal growth of ettringite [4] results in expansive pressure [7,8], which causes the formation of cracks [7]. It appears that the expansion increases with increasing fraction of ettringite formed topochemically and exhibiting oriented growth [9]. Moreover, the ettringite–expansion relationship appears to be related to the curing conditions and on the phase serving as  $\text{Al}^{3+}$  source [9]. The reaction mechanisms involved apparently also depend on the  $\text{Al}_2\text{O}_3$  content of the cement [10,11]. The sulfate concentration of the solution, as well as the aluminate availability, appears to determine the forma-

\* Corresponding author. Materials Science and Engineering Department, Ohio State University, 477 Watts Hall, 2041 College Road, Columbus, OH 43210-1178, USA. Tel.: +1-614-292-2749; fax: +1-614-292-9857.

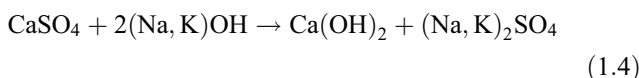
E-mail address: paglia@er6sl.eng.ohio-state.edu (C. Paglia).

tion of gypsum or ettringite [10]. Softening and disintegration were also attributed to gypsum [12], whereas its contribution to expansion remains unclear [13,14]. In fact, Metha [13] claims a relationship between gypsum and expansion, while Hansen [14] contradicts the expansion–gypsum correlation. In recent investigations, however, it was claimed that gypsum may cause expansion [15].

Being the shotcrete in tunnels partially exposed to high temperature, the investigations were carried out at 23 and 65 °C in order to clarify the effect of a temperature increase on the sulfate resistance. High temperature ( $\leq 40$  °C) has been reported to have a deleterious effects on the sulfate resistance of ordinary Portland cement (OPC) [16,17]. At higher temperatures ( $\geq 40$  °C), the diffusion rate of sulfate ions is apparently lowered [17], the solubility of CH is reduced, and the solubility products of ettringite and gypsum are modified [7]. The sulfate and aluminate ions are easily adsorbed with a reversible process on the CSH surface, although the mechanism remains partially unclear. When the temperature decreases, the adsorbed ions pass into the solution and delayed ettringite formation takes place [6,18,19]. Ettringite is stable in deionized water up to 100–130 °C [20,21]. The alkalis seem to reduce the stability [21,22] until ca. 60–80 °C according to Eq. (1.3).



At ca. 80 °C and higher  $\text{OH}^-$  concentration, calcium aluminate hydrates form. At higher  $\text{OH}^-$  concentration, the intermediate  $\text{CaSO}_4$ , formed through the decomposition of ettringite, reacts to CH and  $\text{Na}_2\text{SO}_4$  (Eq. (1.4)).



At room temperature, the reaction is shifted towards  $\text{CaSO}_4$  and consequently towards ettringite formation [21].

Thus, the main goal of the present work is to determine the sulfate attack mechanisms of cementitious material accelerated with alkali-free and alkali-rich admixtures and immersed in  $\text{Na}_2\text{SO}_4$  solutions at 23 and 65 °C.

## 2. Experimental

### 2.1. Admixtures and dosage

The accelerators consisted of alkali-free accelerating substances based on a powdery calciumsulfoaluminate with the addition of powdery  $\text{Al}_2(\text{SO}_4)_3 \cdot 18\text{H}_2\text{O}$  as main components (CSA/SA), and a  $\text{Al}_2(\text{SO}_4)_3 \cdot 18\text{H}_2\text{O}$ -based viscous solution (SA). The alkaline accelerator (AR) consisted of a  $\text{KAl}(\text{OH})_4$  aqueous solution. The dosage refers to the

cement weight and was 6% for the alkali-free accelerator CSA/SA, 8% for the alkali-free accelerator SA and 4.5% for the admixture AR. The plasticizer (Sikatard 902) was based on a sodium carboxylate polysulfonate aqueous solution and was admixed with a dosage of 1%.

### 2.2. Mixing procedure and curing

Cement pastes were prepared by adding water previously mixed with the plasticizer to the cement powder. The accelerators were added after 3 min of mixing. The cement pastes and the accelerators were then mixed for further 45 s. In order to clarify the influence on the expansion, the calciumsulfoaluminate-based alkali-free accelerator was homogeneously (CSA/SA) and inhomogeneously (CSA/SA2) admixed. The inhomogeneous mixing was achieved by adding the accelerator after 3 min of mixing and further mixed for 45 s (“wet mixing procedure”). The homogeneous mixing was carried out by dry mixing the accelerator with the cement powder for 1 min. Water was then added and the mixing procedure was stopped after 3 min and 45 s (“dry mixing procedure”). The cement used was an OPC CEM I 42.5. The total water/cement ratio (including the water content of the accelerating admixtures) was held at 0.46.

All the specimens were immersed in deionized water and in 5%  $\text{Na}_2\text{SO}_4$  ( $\text{Na}_2\text{SO}_4$  powder 99.5%) solution at 23 °C and at 65 °C up to 6 months. The solutions were not renewed during the time of exposure, since generally the time to failure of the specimens, in particular at 65 °C, was very short ( $< 60$  days). Thus, the slight long-term variations in the  $\text{SO}_4^{2-}$  concentration (23 °C, 65 °C) were considered to exert a negligible effect on the main attack. The solution/specimen volume ratio was also considered high enough to avoid a significant influence of the change in solution chemistry on the sulfate attack. The specimens were not placed in a saturated lime solution in order to increase the porosity due to the CH leaching. In this manner, a faster response to the sulfate resistance in the laboratory was obtained. The solutions were not stirred during this time.

### 2.3. Investigation techniques

#### 2.3.1. Length change

Cement pastes were cast in polystyrene  $120 \times 120 \times 120$  mm forms. After demoulding (1 day) and storage for 56 days in deionized water at 23 °C, cylindrical specimens (100 mm length–50 mm diameter) were prepared and bolts were glued at the edges. The number of test specimens ranged between 5 and 6 for a specified accelerator and curing condition. The specimens were placed vertically in a plastic box with a grid at the bottom to allow homogeneous contact with the solution. The volume of water or sulfate solution was on average 26 l. The measurements were performed weekly up to 28 days and every 2 weeks up to 6 months (ASTM C 1012-95). The netto linear expansions were measured from the difference between the sulfate and the water-cured specimens.

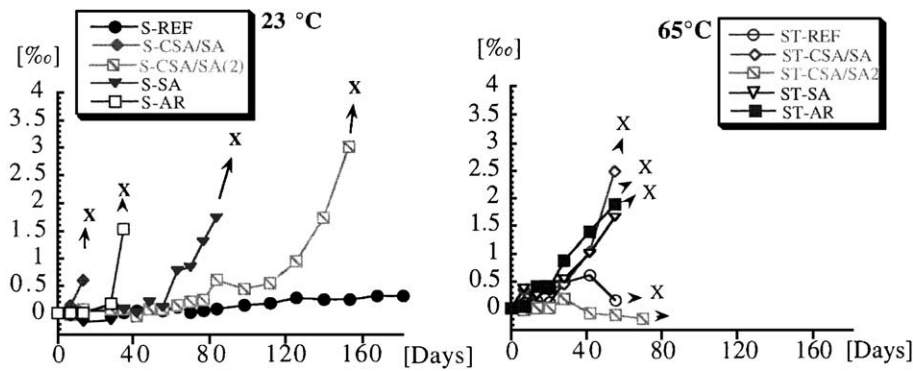


Fig. 1. Linear expansion of the specimens. Left: 23 °C. Right 65 °C. The notation “X” indicates the complete disruption. The values indicate the difference between sulfate and water-cured specimens.

2.3.2. X-ray diffraction

Cement paste disks were pulverised (63 µm) along the exposed borders (4 mm depth) and an internal standard (20% boehmite) was admixed. The measurements were carried out after 1, 7, 14, 21, 28, 56, 91, and 182 days with a Philips APD 1900 X-ray diffractometer using CuKα (λ = 1.5405 nm) radiation (30 mA, 40 kV). A quantitative Rietveld analysis [23] was performed using an Autoquan 2.0.0.0 software cernel routine BGMN with boehmite as internal standard. The phases formed were obtained from

the difference between the sulfate and the water-cured specimens.

2.3.3. Ion chromatography (IC)

Cylindrical cement paste specimens (100 mm length × 50 mm diameter) were covered with an epoxy resin and cut along the longitudinal side to allow a unidimensional attack. After 28 and 91 days, the exposed surface was pulverised down to 5 mm (step of 1 mm each). The cementitious powder was collected in tight plastic contain-

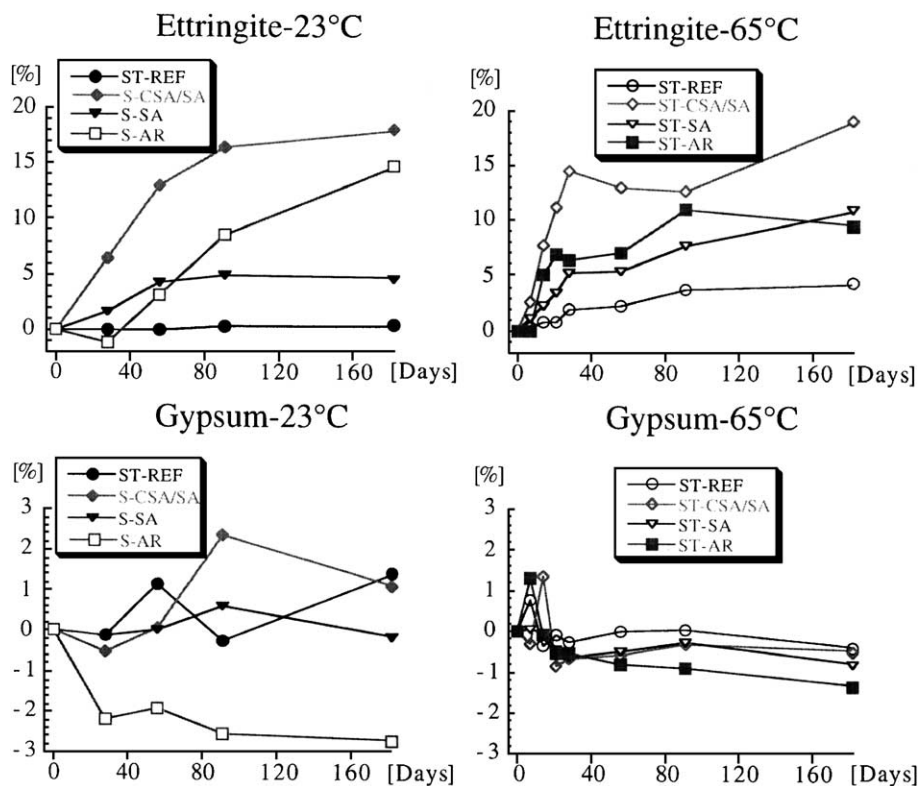


Fig. 2. XRD data. Development of ettringite and gypsum at 23 °C and at 65 °C during time. The data indicate the difference between sulfate and water-cured specimens. Average Rwp 12.42% (Rietveld method: fitting quality).

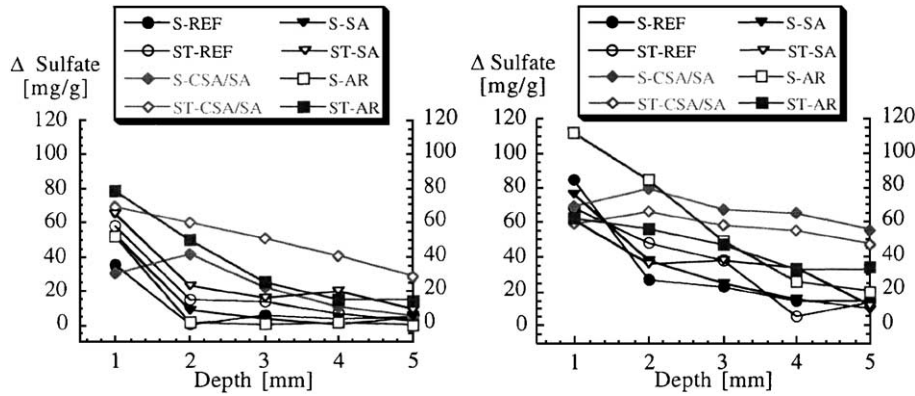


Fig. 3. IC measurements: penetration depth vs. total adsorbed sulfate at 23 and 65 °C after 28 days (left), and 91 days of curing (right). The data indicate the difference between sulfate and water-cured specimens.

ers. Suspensions of 0.50 g powder, 40 ml deionized water, and 10 ml HCl (0.5 M) were prepared for each mixture type, curing condition and for each millimeter depth down to 5 mm. The filtered solutions were measured with a Metrohm Ion Chromatograph. The working conditions were set at 2000 μl/min, 20 °C and 79 bar. The eluent consisted of a solution of 2 mM phthalic acid/10% acetone/pH 5.0. The dilution was 1:100 and the standard calibration solution had a concentration of 200 μM sulfate ions. The quantitative evaluation was performed with a Custom IC-metrodata

for windows Metrohm. The sulfate present resulted from the differences between the specimens prior and after sulfate curing.

2.3.4. pH

Filtered suspensions prepared as described for the IC measurements, but without HCl, were measured after 28 and 91 days of exposure (water and sulfate) with an Orion 960 Autochemistry system consisting of an Orion 960 Module and an EA 940 pH/ISE Meter.

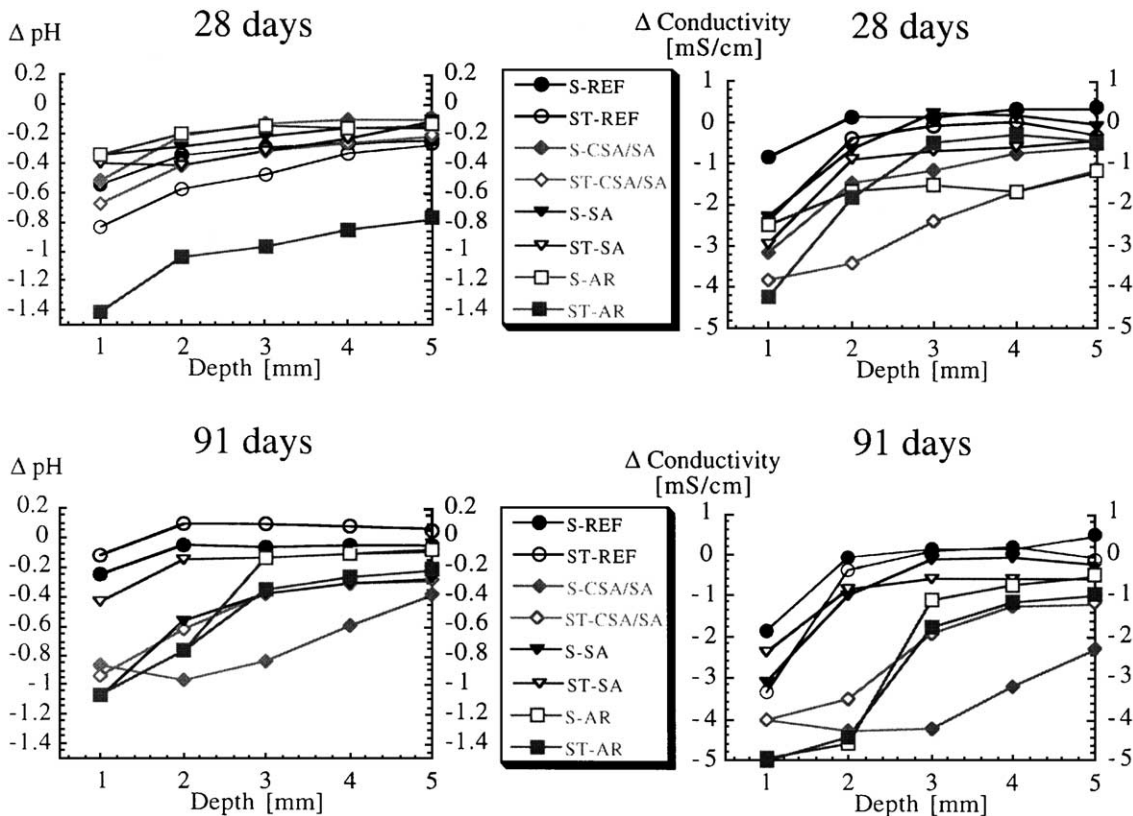


Fig. 4. pH (left side) and conductivity (right side) of the solution of the mixtures cured at 23 and 65 °C for 28 and 91 days. The data are relative and reflect the difference in conductivity and pH between the sulfate and water-cured specimens.

### 2.3.5. Conductivity

Filtered suspensions prepared as described for the IC measurements, but without HCl, were measured after 28 and 91 days exposure (water and sulfate) with an auto range CDM 83 Conductivity Meter.

### 2.3.6. Scanning electron microscopy

The investigations were carried out within the external surface layers of the cement paste disks cut from the cylindrical specimens after 56 days of sulfate exposure. The sample surfaces were dried for 4 h at  $10^{-2}$  Torr. After further drying at  $5 \times 10^{-2}$  mbar for 24 h, the samples were coated with gold and were examined with a conventional JEOL JSM 840 equipped with a Tracor Microtrace TM Silicon X-ray Spectrometer with Pulsed Optical Feedback Preamplifier 505 and a Tracor software system. The accelerating voltage was kept at 20 kV.

## 3. Results and analysis

### 3.1. Dimensional stability

At 23 °C, the homogeneously distributed calciumsulfoaluminate-based alkali-free accelerator shows the fastest expansion (Fig. 1, S-CSA/SA). The inhomogeneous dissolution of the alkali-free accelerator (Fig. 1, S-SA) and the inhomogeneously distributed calciumsulfoaluminate-based alkali-free admixture (Fig. 1, S-CSA/SA2), cause a delay in the expansion. The expansion of the samples accelerated with the alkaline admixture occurs at early ages (Fig. 1, S-AR), while the unaccelerated samples (Fig. 1, S-REF) exhibit a slight expansion up to 6 months.

At 65 °C, the homogeneously distributed calciumsulfoaluminate-based alkali-free accelerator delays the expansion (Fig. 1, ST-CSA/SA). Up to 6 months, the inhomogeneously

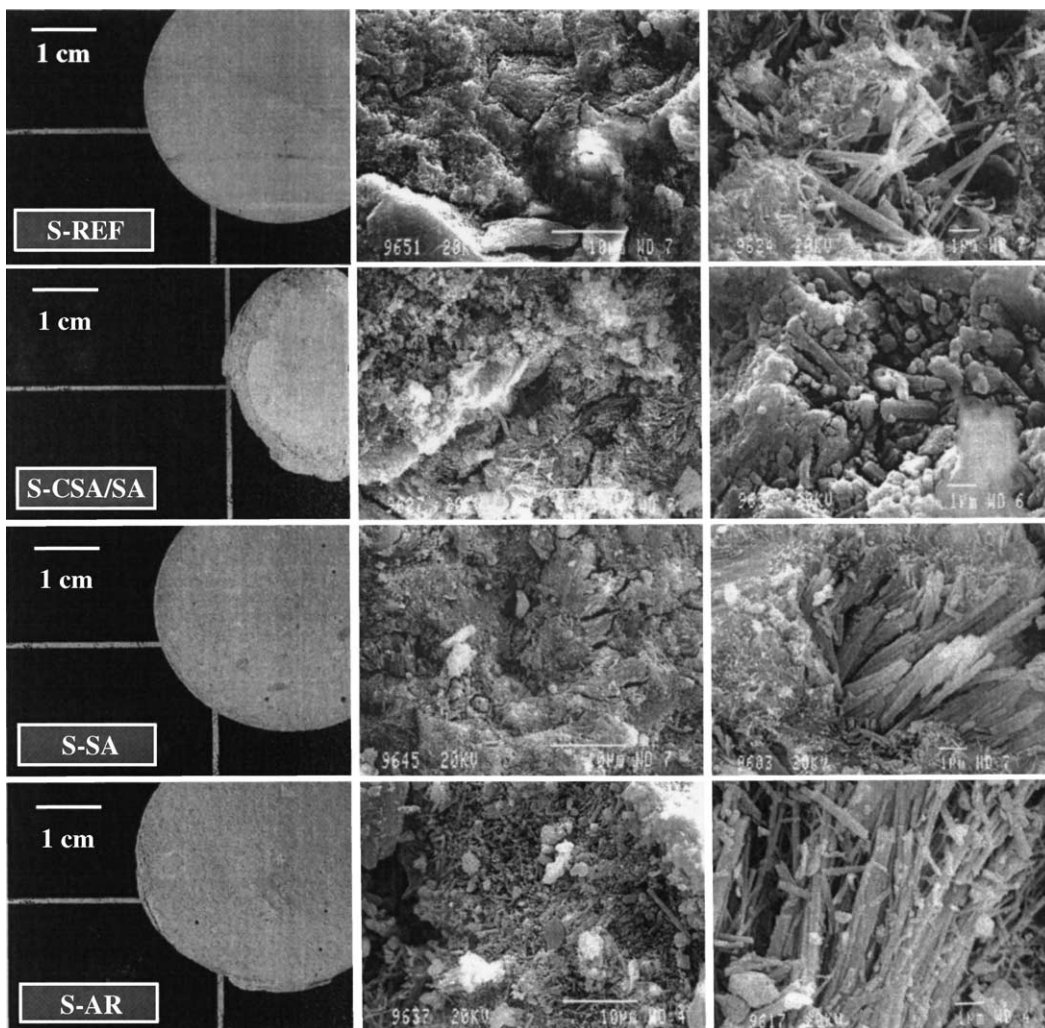


Fig. 5. Damage (left) vs. microstructural features of the exposed layers (center magn. 2500–right magn. 10000) of the specimens cured for 56 days at 23 °C.

distributed calciumsulfoaluminate-based alkali-free accelerated samples do not expand (Fig. 1, ST-CSA/SA2), while the inhomogeneous addition of the alkali-free admixture shows a slightly accelerated expansion (Fig. 1, ST-SA). The alkaline accelerated samples exhibit lower length changes (Fig. 1, ST-AR), while the unaccelerated samples (Fig. 1, ST-REF) strongly accelerate their expansion.

### 3.2. Main phases development

At 23 °C, the amount of gypsum detected by XRD generally fluctuates, but appears to increase for the alkali-free (Fig. 2, S-CSA/SA; S-SA) and the unaccelerated samples (Fig. 2, S-REF). On the other hand, the samples accelerated with the alkaline admixture exhibit declining gypsum values (Fig. 2, S-AR). Generally increased ettringite amounts are observed at 65 °C within the first 28 days, although for the calciumsulfoaluminate-based alkali-free accelerated samples (Fig. 2, ST-CSA/SA) and the alkaline type (Fig. 2 ST-AR), a reduction in the ettringite amount is observed at later stages. At 65 °C, gypsum exhibits an

increase in the amount at early stage (<15 days), although at a later stage, declining gypsum contents are observed (Fig. 2). This paradoxically indicates that lower crystalline gypsum amounts are detected for the samples after the exposure to sulfate solution as compared to water curing.

### 3.3. Diffusion of sulfate ions

The ion chromatographic measurements indicate a higher sulfate adsorption for the accelerated specimens compared to the unaccelerated samples at 23 and 65 °C. At 65 °C, generally increased sulfate amounts are observed (Fig. 3), although up to 91 days and at 23 °C, higher adsorption of sulfate ions are observed for the samples accelerated with the calciumsulfoaluminate-based, the alkali-free and the alkaline admixture at 23 °C (Fig. 3, S-CSA/SA; S-SA; S-AR). After 28 days of sulfate exposure, a high sulfate adsorption is generally observed within the first 2 mm of the exposed surfaces. Up to 91 days, the sulfate amounts generally increase and reach in particular for the calciumsulfoaluminate-based alkali-free accelerated samples con-

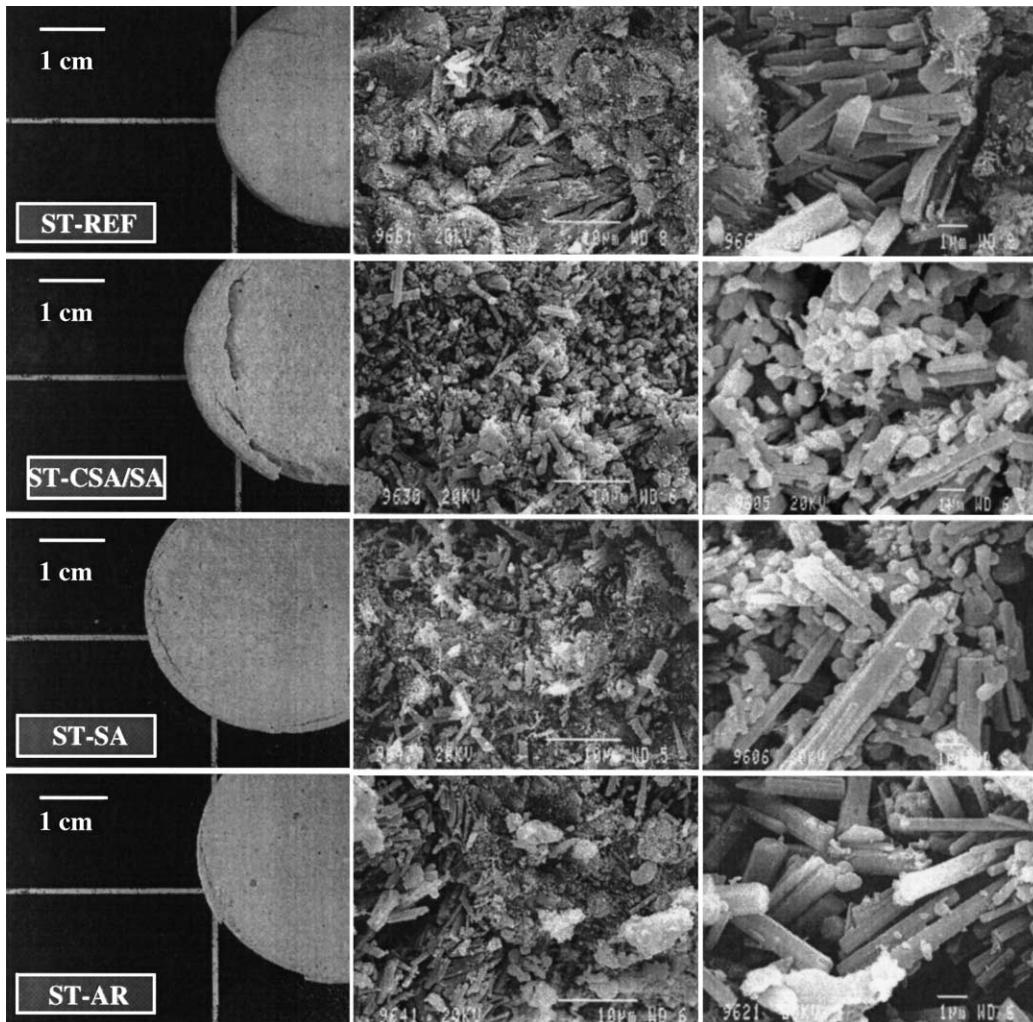


Fig. 6. Damage (left) vs. microstructural features of the exposed layers (center magn. 2500–right magn. 10000) of the specimens cured for 56 days at 65 °C.

stant high values along the entire profile down to 5 mm (Fig. 3, S-CSA/SA; ST-CSA/SA).

### 3.4. The exchange $SO_4^{2-} \rightleftharpoons OH^-$

Microstructural observations of the  $MgSO_4$  attack allowed a representation of a counter-diffusion pattern of  $OH^-$  ions from the specimens outward and  $SO_4^{2-}$  from the solution inward [24]. The same counter-diffusion process is assumed in this work for the  $Na_2SO_4$  attack. Because of the different mobility of the  $OH^-$  ions ( $20.52 \times 10^{-4} \text{ cm}^2/\text{s/V}$ ) and  $SO_4^{2-}$  ions ( $8.27 \times 10^{-4} \text{ cm}^2/\text{s/V}$ ) ions, pH and conductivity measurements were taken as a measure of the  $SO_4^{2-} \rightleftharpoons OH^-$  exchange, i.e. of the sulfate penetration. The higher the ions exchange, the larger the drop in the conductivity and in the pH value of the solutions. Generally, the highest  $SO_4^{2-} \rightleftharpoons OH^-$  exchange during time is observed for the samples accelerated with the calciumsulfoaluminate-based alkali-free admixture at 23 and 65 °C (Fig. 4, S-CSA/SA; ST-CSA/SA). The conductivity measurements, however, indicate a better discrimination between the samples as compared to the pH measurements (Fig. 4).

### 3.5. Structural damage of the exposed layers

The unaccelerated samples exhibit no damage of the exposed surface layers with a high presence of the CSH amorphous dense gel and ettringite prisms (5  $\mu\text{m}$ ) occasionally precipitated within the pores (Fig. 5, S-REF). The specimens with the homogeneously distributed calciumsulfoaluminate-based alkali-free accelerator show a complete softening of the specimens with the disintegration of the CSH gel and a general increase in the porosity. Elongated ettringite crystals are largely present (Fig. 5, S-CSA/SA). A bad homogenization of the alkali-free accelerator results in a slight disruption and cracking. The dense CSH gel is largely observed and ettringite-enriched zones are occasionally present and form the white efflorescences on the specimen surface (Fig. 5, S-SA). The addition of the alkaline admixture causes a spalling and cracking of the surface layer, which mainly consists of tightly packed ettringite bundles (Fig. 5, S-AR).

At 65 °C, ettringite prisms fill the pores of the unaccelerated samples which exhibits a slight disruption (Fig. 6, ST-REF). The addition of the homogeneously distributed calciumsulfoaluminate-based alkali-free accelerator indicates a moderate softening of the samples. The CSH gel is slightly present and short ettringite prisms are observed (Fig. 6, ST-CSA/SA). The inhomogeneous distribution of the alkali-free accelerator indicates an initial cracking of the exposed surface layer and the presence of both long and short prismatic ettringites (Fig. 6, ST-SA). The addition of the alkaline admixture results in the initial spalling and cracking of the surface layer which mainly consists of big ettringite prisms with a high porosity in-between (Fig. 6, ST-AR). CSH gel is also occasionally observed.

## 4. Discussion

### 4.1. Attack mechanisms and physical consequences

A direct correlation between ettringite and expansion is not always evident. A correlation between ettringite formation and expansion can be associated with the precipitation of ettringite crystals, which fill the pores and exert a pressure against the neighbouring hydrated mass causing expansion. In this latter case, ettringite precipitation takes place with a supersaturation of the pore solution with respect to  $Al^{3+}$ ,  $SO_4^{2-}$  and  $Ca^{2+}$  ions. Despite the high presence of CH supplied during cement paste hydration [25], microstructural investigations, as well as the characterization of the damage type, indicate a decalcification of the CSH gel with a resulting softening of the specimens. The  $Al^{3+}$  and  $SO_4^{2-}$  ions introduced with the alkali-free admixtures appear to promote the decalcification process, in particular, when the accelerator is homogeneously admixed within the cementitious mass. In this latter case, increased deleterious effects are observed. The decalcification of the CSH gel is presumably due to the high consumption of the  $Ca^{2+}$  and  $OH^-$  ions during ettringite formation [26]. In fact, the ettringite formation process is particularly promoted with the addition of the alkali-free admixture homogeneously distributed within the cementitious mass. Thus, CSH decalcification takes place in spite of the generally high presence of  $Ca^{2+}$  and  $OH^-$  ions within the pore solution [25]. The presence of sulfate ions also causes a local pH decrease. In order to re-establish the high pH required for the CSH gel stability (13–13.5), lime is liberated from the CSH gel. As a consequence, softening of the whole structure occurs. Although the disintegration process does not proceed to completion, as it does for the  $MgSO_4$  solutions [10,11,24,27], an attack of the CSH gel takes place within the investigated samples stored in  $Na_2SO_4$  solutions. The decalcification of the CSH gel generally increases the porosity of the specimens. The risen porosity promotes an increased penetration and adsorption of sulfate solution as confirmed by IC, pH, and conductivity measurements. The increased penetration of solution results in an additional swelling of the specimens, which directly contributes to the expansion and presumably explains the lack of a direct relationship between the ettringite and the expansion observed in this work. This latter mechanism mainly occurs when the CSA-based alkali-free accelerator is homogeneously admixed (CSA/SA).

An inhomogeneous distribution of the alkali-free admixtures (CSA/SA2; SA) reduces the ettringite amount and the CSH gel decalcification which takes place only at isolated sites. The samples exhibit a delayed expansion and damage and tend to disrupt rather than disintegrate, due to the remaining high presence of a CSH gel framework, which supports the cohesion of the samples.

When the alkaline accelerator is used, large amounts of platy CH crystallize within the pores [28]. Despite the

presence of aluminates homogeneously distributed within the mixture, the  $\text{Ca}^{2+}$  and  $\text{OH}^-$  ions additionally available within the pore solution act as  $\text{Ca}^{2+}$  supplier as opposed to the CSH gel. The high basicity of the alkaline admixture also reduces the likelihood of a local pH decreases due to the sulfate ions penetration, so that the CSH is additionally protected from the decalcification process. The high availability of CH and aluminates within the pores causes the rapid formation of tightly packed ettringite bundles, which cause the expansion and the spalling of the surface layers.

Generally, the  $\text{Al}^{3+}$  and  $\text{SO}_4^{2-}$  additionally introduced via the admixtures promote, under the specific experimental conditions, an attack mechanism and damage typical for  $\text{MgSO}_4$  attack, namely, the CSH decalcification which results in the softening of the specimens. The extent of the damage, however, depends on the homogeneization of the accelerating admixture within the cementitious mass.

A direct contribution of gypsum to the expansion at 23 and 65 °C could not be clearly determined with the investigations techniques performed in this work. However, it is believed that due to the additional aluminate and sulfate introduced via the admixtures, and the low gypsum presence detected by XRD as compared to ettringite, the damage mechanisms are mainly controlled by the ettringite formation.

#### 4.2. Influence of the higher temperature

At 65 °C, the reactions are generally accelerated. Mangat and El-Khatib [16] reported an ettringite crystal growth (<28 days) even at  $T < 40$  °C. An increase in the ettringite size and an increase in the  $\text{SO}_4^{2-}$  adsorption take place and contribute to fill the capillary pores. These latter processes generally occur in the unaccelerated samples and within the samples with an inhomogeneous distribution of the alkali-free admixtures, i.e. with an inhomogeneous distribution of the aluminate–sulfate enrichments. In these cases, the CSH gel is poorly attacked, and the restrained growth of the ettringite exerts the pressure to a maximum extent, increasing the cracking and disruption.

At later ages (>28 days), the ettringites become generally unstable and recrystallize to a smaller size with a less defined crystal shape. The decrease in the ettringite crystal size presumably delays the expansion and the disintegration of the alkali-free accelerated samples (CSA/SA). Furthermore, the CSH gel is generally less prone to decalcification and more  $\text{SO}_4^{2-}$  and  $\text{Al}(\text{OH})_4^-$  can be adsorbed on its surface [22]. However, microstructural investigations indicate in some areas a decalcification of the CSH gel and the presence of ettringite. The ettringite formation presumably initiates when  $\text{SO}_4^{2-}$  ions come in contact with the aluminate-rich sites on the CSH gel surface, but it is slightly different from the conventional delayed ettringite formation mechanism [6,18,19].

The delayed expansion and damage of the samples accelerated with the alkaline admixture is mainly related

to the rearrangement and accommodation of the ettringite crystals. In fact, the increased ettringite dimensions force them to be accommodated with big pores in-between rather than as tightly packed bundles. The high presence of the CSH gel confirms its increased ion adsorption capacity. The  $\text{Ca}^{2+}$  necessary to form the higher initial amounts of ettringite appears to be mainly supplied by the dissolution of the CH crystals, in spite of their lower solubility at high temperatures [7]. This prevents the CSH gel to act as  $\text{Ca}^{2+}$  supplier, avoiding its disintegration. The alkalis generally reduce the thermal stability of ettringite [21,22] but within the investigated alkali-rich accelerated cementitious system, the alkalis added via the admixture play a subordinate role in the ettringite thermal stability.

## 5. Conclusions

- The damage (softening and disintegration, disruption and cracking) was largely controlled by the presence of  $\text{Al}^{3+}$  and  $\text{SO}_4^{2-}$  ions, which controlled the extent of the CSH gel decalcification. The  $\text{Al}^{3+}$  and  $\text{SO}_4^{2-}$  ions supply was largely related to the homogenization of the admixtures within the cementitious mass.
- The extent of the CSH gel decalcification was mainly controlled by the presence and distribution of the aluminates, sulfates, and the CH availability.
- The enhanced porosity resulting from the CSH gel decalcification promoted the further absorption of the sulfate solution, which partially contributed to the expansion. This latter process presumably explains the lack of a direct relationship between ettringite and expansion.
- The increase in the temperature had a variable effect in the extent of the damage, which depended on the  $\text{Al}^{3+}$  and  $\text{SO}_4^{2-}$  availability, crystal rearrangements, ion adsorption capacity of the CSH gel, and on the thermal instability of ettringite.

## Acknowledgements

This work was supported by SIKA Zurich Switzerland and the Institute of Materials Chemistry and Corrosion ETH-Zurich, Switzerland.

## References

- [1] D. Mai, Advanced Experiences with High Performance Alkali-Free Non-Toxic Powder Accelerator for All Shotcrete Systems, presented at Sprayed Concrete Technology for the 21st Century, Edinburgh, 1996.
- [2] H. Huber, J. Gantner, W. Kusterle, Spritzbeton mit Alkalifreier Erstarungsbeschleunigung—Umweltneutraler Spritzbeton, *Zem. Beton* 1 (1994) 19–21.
- [3] C. Ouyang, A. Nanni, W.F. Chang, Internal and external sources of sulfate ions in portland cement mortar: Two types of chemical attack, *Cem. Concr. Res.* 18 (1988) 669–709.

- [4] B. Wicht, J. Stark, Dauerhaftigkeit von Beton 100, FIB F.A. Finger-Institut für Baustoffkunde, Weimar, 1995.
- [5] N.J. Crammond, Examination of mortars bars containing varying percentages of coarsely crystalline gypsum as aggregate, *Cem. Concr. Res.* 14 (1984) 225–230.
- [6] A.W. Klemm, F.M. Miller, Plausibility of delayed ettringite formation as a distress mechanism, Considerations at Ambient and Elevated Temperatures, Proceedings of the 10th International Congress on the Chemistry of Cement, vol. 4, Amarkai AB and Congrex, Gothenburg, Sweden, 1997, 10 pp., 4iv059.
- [7] X. Ping, J.J. Beaudoin, Mechanism of sulphate expansion: II. Validation of thermodynamic theory, *Cem. Concr. Res.* 22 (1992) 845–854.
- [8] X. Ping, J.J. Beaudoin, Mechanism of sulphate expansion: I. Thermodynamic principle of crystallization pressure, *Cem. Concr. Res.* 22 (1992) 631–640.
- [9] I. Odler, J. Colan-Subauste, Investigations on cement expansion associated with ettringite formation, *Cem. Concr. Res.* 29 (1999) 731–735.
- [10] R.S. Gollop, H.F.W. Taylor, Microstructural and microanalytical studies of sulfate attack: III. Sulfate-resisting portland cement. Reactions with sodium and magnesium sulfate solutions, *Cem. Concr. Res.* 25 (1995) 1581–1590.
- [11] R.S. Gollop, H.F.W. Taylor, Microstructural and microanalytical studies of sulfate attack: V. Comparison of different slag blends, *Cem. Concr. Res.* 26 (1996) 1029–1044.
- [12] J.G. Wang, Sulfate attack on hardened cement paste, *Cem. Concr. Res.* 24 (1994) 735–742.
- [13] P.K. Metha, Sulfate attack on concrete—a critical review, *Materials Science of Concrete III*, American Ceramic Society, Westerville, OH, 1992.
- [14] W.C. Hansen, Crystal growth as a source of expansion in portland cement concrete, *Proc. Am. Soc. Test. Mater.* 63 (1963) 932–945.
- [15] B. Tian, M.D. Cohen, Does gypsum formation during sulfate attack on concrete lead to expansion? *Cem. Concr. Res.* 30 (2000) 117–123.
- [16] P.S. Mangat, J.M. El-Khatib, Influence of initial curing on sulphate resistance of blended cement concrete, *Cem. Concr. Res.* 22 (1992) 1089–1100.
- [17] A. Fevziye, F. Türker, S. Koral, N. Yüzer, Effects of raised temperature of sulfate solutions on the sulfate resistance of mortars with and without silica fume, *Cem. Concr. Res.* 29 (1999) 537–544.
- [18] B. Lagerblad, P. Utkin, The effect of water–cement ratio, sulphonated plasticizer and silica fume on delayed ettringite expansion, presented at Durability of High Performance Concrete, Proceeding of the RILEM International Workshop, Vienna, 1994.
- [19] S. Kelham, Effects of cement composition and hydration temperature on volume stability of mortar, Proceeding of the 10th International Congress on the Chemistry of Cement, vol. 4, Amarkai AB and Congrex, Gothenburg, Sweden, 1997, 8 pp., 4iv060.
- [20] K. Ogawa, D.M. Roy,  $C_4A_3S$  hydration, ettringite formation, and its expansion mechanism: I. Expansion; ettringite stability, *Cem. Concr. Res.* 11 (1981) 741–750.
- [21] W. Wieker, C. Hübert, H. Schubert, R. Herr, Sekundäre Ettringitbildung und ihre Bedeutung für die Dauerhaftigkeit, *BMI 1* (1997) 107–112.
- [22] L. Divet, R. Randriambololona, Delayed ettringite formation: The effect of temperature and basicity on the interaction of sulphate and CSH phase, *Cem. Concr. Res.* 28 (1998) 357–363.
- [23] R.A. Young, The Rietveld method, *IUCr Monogr. Crystallogr.* 298 (1993).
- [24] D. Bonen, M.D. Cohen, Magnesium sulfate attack on portland cement paste: II. Chemical and mineralogical analysis, *Cem. Concr. Res.* 22 (1992) 707–718.
- [25] Tricalcium silicate (Section 6.2.1), in: P.C. Hewlett (Ed.), *Lea's Chemistry of Cement and Concrete*, 4th ed., Arnold, London, 1998, p. 246.
- [26] Kinetics of the hydration process (Section 6.4.3), in: P.C. Hewlett (Ed.), *Lea's Chemistry of Cement and Concrete*, 4th ed., Arnold, London, 1998, p. 269.
- [27] D. Menashi, A. Bentur, Durability of portland–silica fume pastes in magnesium sulfate and sodium sulfate solutions, *ACI Mater. J.* 85-M18 (1988) 148–157.
- [28] C. Paglia, F. Wombacher, H. Boehni, The influence of alkali-free and alkaline shotcrete accelerators within cement systems: I. Characterization of the setting behavior, *Cem. Concr. Res.* 31 (2001) 913–918.